

# We are IntechOpen, the world's leading publisher of Open Access books Built by scientists, for scientists

5,300

Open access books available

130,000

International authors and editors

155M

Downloads

Our authors are among the

154

Countries delivered to

TOP 1%

most cited scientists

12.2%

Contributors from top 500 universities



WEB OF SCIENCE™

Selection of our books indexed in the Book Citation Index  
in Web of Science™ Core Collection (BKCI)

Interested in publishing with us?  
Contact [book.department@intechopen.com](mailto:book.department@intechopen.com)

Numbers displayed above are based on latest data collected.  
For more information visit [www.intechopen.com](http://www.intechopen.com)



---

# Active and Passive Acoustic Methods for In-situ Monitoring of the Ocean Status

---

Sara Pensieri and Roberto Bozzano

Additional information is available at the end of the chapter

<http://dx.doi.org/10.5772/intechopen.68998>

---

## Abstract

Recent European strategic plans for the successful monitoring of the status of the ocean push on the development of an integrated observing system able to further link existing instruments and techniques with the aim to complement each other and answer open issues. A more intensive use of acoustic devices could contribute to the knowledge of oceanographic processes exploiting the characteristic of sound to travel in the ocean for a wide area than in the atmosphere. In this context, the installation of passive acoustic instruments, able to listen to ambient noise on fixed or mobile platforms, could contribute to provide information on sound budget and to enhance the monitoring capacity of meteorological phenomena also in the open ocean. Instead, the deployment of active acoustic instruments can be of benefit for monitoring biological activities through the analysis of backscatter data as well as for monitoring ocean waves.

**Keywords:** active underwater acoustics, ocean passive underwater acoustic, underwater ambient noise, oceanography, in-situ monitoring

---

## 1. Introduction

A fully comprehensive picture of the ocean status can be obtained only by combining different methods and monitoring techniques exploiting the characteristics of each approach. The recent enhancement of remote sensing capabilities, in terms of a variety of measured parameters and accuracy of the corresponding estimates, has been contributing to an effective improvement of the skill of forecasting models and, generally speaking, to the whole domain of operational oceanography which also benefits in real-time measurements provided by equipped buoys, moorings, and mobile platforms (floats, AUV, glider, etc.) that represent the principal resources to acquire in-situ ocean measurements.

---

While methodologies for the monitoring of the physical properties of the ocean are fully assessed and guarantee a good spatial and temporal coverage, techniques to monitor biochemical processes as well as meteorological phenomena over the ocean are still open issues [1].

Underwater acoustic systems, both active and passive, could contribute to fill this gap by listening to the ocean noise or by transmitting pulses and interpreting the received echoes to improve the knowledge on biological activities or meteorological phenomena at sea such as rain and wind and the potential harmful impact of human activities on the ecosystem.

The feasibility of using underwater acoustics to propagate signals date back to 1918 but only during the Second World War there was a massive exploitation of devices to detect submarines through sound navigation and ranging system (sonar). The first civilian experiments to measure the sea bottom and to detect schools of fishes were carried out in the first half of the twentieth century [2]. Since then, the benefits of underwater acoustics were proportional to the technological developments in both hardware and software components, especially for oceanographic applications.

Several aspects have to be taken into account when planning an underwater acoustics measurement program. The most important factor is the type of noise being measured and, accordingly, its expected features in terms of amplitude, frequency, duration, and so on, which drive the choice of measurement equipment. Indeed, the sound in the ocean is characterized by speed of propagation, attenuation, and presence of obstacles along the path and by the way in which the sound is scattered, backscattered, and refracted by both the bottom and the surface.

Ocean stratification is the main responsible event for the generation of beams (convergent and/or divergent) and grey areas, depending on the change in the speed due to the depth. In turn, sea temperature profiles are influenced by diurnal cycle, season, and weather conditions. During winter months, the surface water that is colder and saltier tends to sink, and it is replaced by warmer and deeper water masses. This mixing could originate a layer of isotherm water characterized by a homogeneous sound velocity defined as "mixed layer." Below, the thermocline, that is the area in which temperature rapidly decreases with depth, dwells. The mixing of the water column implies an enlargement of the mixed layer and an erosion of the thermocline. The layer below the thermocline is characterized by a quite constant temperature and presents a minimum in the sound speed profile.

In the ocean, sound pressure levels (SPL) are retrieved using the sonar equation (Eq. (1)) as the difference between the transmitted power (SL) and the power loss (TL) through the path [3].

$$SPL [dB] = SL[dB] - TL[dB] = 10 \log \left( \frac{P_0}{P_R} \right)^2 - \left[ 20 \log \left( \frac{R}{R_0} \right) + \alpha(R - R_0) \right] \quad (1)$$

$P_0$  is the pressure of the transmitted signal at a known distance  $R_0$ ,  $P_R$  is the reference pressure (generally equal to 1  $\mu$ Pa), and  $R$  is the distance of the listener from the source.

Equation (1) allows the quantification of SPL acquired by passive devices that simply listen to the numerous and heterogeneous ocean sounds like, among others, those produced by mammals, marine organisms, volcanoes, submarines, human activities, wind, waves, and rain.

Since active instruments are able to transmit a pulse and listen to its echo, it is necessary to consider also the intensity of the echo one meter from the target, that is, relative to the part of the sound that hits the target, the so-called target strength (TS). Thus, Eq. (1) is modified in Eq. (2)

$$SPL [dB] = SL[dB] - 2TL[dB] + TS [dB] = 10 \log \left( \frac{P_0}{P_R} \right)^2 - 2 \left[ 20 \log \left( \frac{R}{R_0} \right) + \alpha(R - R_0) \right] + TS. \quad (2)$$

Among the others types of applications, active instruments are commonly used to detect schools of fish, mines, and currents.

In the design of an acoustic experiment also, the availability, or the construction, of adequate infrastructure for carrying out the measurements for a desired duration is a key requirement. The two most common approaches consist of using mobile and fixed platforms.

In vessel-based surveys, hydrophones (either individually or in arrays) are deployed from the ship, and the analysis and recording equipment remain on the vessel, which may be either anchored or drifting. This solution is relatively easy to implement, the deployments can be quick, a relatively large area may be covered, the risk of losing instrumentation is low, the configuration of hardware devices can be adjusted online, and data can be monitored in real time. Nonetheless, the main disadvantage consists of the pre-defined and limited (usually short) period of time during which the measurements can take place. Also, autonomous moving platforms such as gliders can be equipped with hydrophones to explore the soundscape of relatively large areas of the ocean.

When continuous time monitoring is of interest or when the objective is to observe episodic and non-predictable phenomena (i.e., biological and geological events), a Eulerian approach is preferable. This consists of the use of fixed observatories that can be based on sea bottom stations cabled to the shore [4] or on instruments deployed on oceanic sub-surface moorings [5] or surface buoys. Several large initiatives are currently operational all over the world: Ocean Observatories Initiative (OOI) in the USA, Neptune in Canada, European Seas Observatory NETwork (ESONET), and the neutrino telescope sites in Europe [6]. Cabled observatories allow data to be streamed directly to the shore base and checked in real time [7]. Unless the goal is to measure air-sea surface interactions through acoustics or characterize the acoustic signature of ships, bottom-mounted deployments offer the advantage of minimizing both the influence of surface wave action and the disturbance by surface vessels, reducing the risk to keeping the hydrophone away from the pressure-release water-air surface and the risk of damage to the equipment.

The characterization of the ambient sound all over the world oceans, through the variety of approaches mentioned above, has become more common as interest in the trends in anthropogenic sound in the ocean grows. The European Commission endorsed this issue considering the introduction of energy, including underwater noise, into the ocean as a pollutant [8] and requesting to monitor it with the same operative methodologies like other physical, biological, and chemical parameters.

## 2. Ocean waves statistics inferred by active acoustic devices

### 2.1. Ocean waves

Sea surface shows ripples of different dimensions and shapes, depending on the force of the wind speed, and on the basis of their characteristics, they can be subdivided in two categories: capillary and gravity waves. Ocean capillary waves are strictly connected to surface tension and show short wavelength, whereas ocean gravity waves are due to the force of the air-sea interface conditions and their wavelength can reach several meters, especially in open oceans during storms. The characteristics of the waves, induced by winds, are identifiable by wind speed intensity and distance and by the duration of the event [9, 10].

When energy loss due to the air-sea friction is negligible, waves can propagate until one of these events occur: wind forcing persists, waves are hindered by the presence of dams or consume their energy on the coastline. Dissipations of energy reduce inversely proportional to wavelength; thus, large wavelengths, generally faster, smooth slowly and propagate over long distance even where wind is absent.

Waves induced by wind force can be modeled by Eq. (3) as  $N_w$  sinusoids linearly interact each other, where each component is identified by an own amplitude ( $A_m$ ), wavenumber ( $k_m$ ), direction of propagation ( $\theta_m$ ), frequency ( $f_m$ ), and initial phase ( $\varphi_m$ ).

$$z(t) = \sum_{m=1}^{N_w} A_m \cos [k_m (x \cos \theta_m - y \sin \theta_m) - 2\pi f_m t + \varphi_m] \quad (3)$$

where  $x$  is the displacement along  $x$  axes,  $y$  the displacement along  $y$  axes, and  $\varphi$  is a random uniformly distributed variable between  $-\pi$  and  $\pi$ . Sinusoidal waves with different frequencies propagate with the same speed related to bottom depth in shallow water, whereas they have a decreasing speed as the frequency rises in open ocean.

Wind blowing for an extended period of time over a long distance induces a rapid increase of both wave steepness and height. The upper limit of the height is reached when wave breaking generates a dissipation of energy able to balance the energy supplied by wind and, in this case, wave motion can be considered as fully developed. Each component of fully developed waves is a random ergodic process characterized by a variance equal to the mean quadratic value  $A_m^2/2$ . The variance of the whole wave field can be expressed as a summation of the  $N_w$  components in the  $\Delta f$  frequency band through Eq. (4) and it represents the monolateral power spectra.

$$S(f) = \frac{1}{2} \frac{\sum_{m=1}^{N_w} A_m^2}{\Delta f} \quad (4)$$

Through the 0th and 1st spectral moments of  $S(f)$ , it is possible to estimate the main characteristics of ocean waves. In fact, the mean pulse is the ratio between the 1st moment and the 0th moment, whereas the mean period is obtained dividing  $2\pi$  by the mean pulse. The significant wave height can be defined as the average height of one-third of the highest measured waves ( $H_{1/3}$ ) and can be expressed as 4.005 times the root square of the 0th moment [11].

## 2.2. Measuring ocean waves with acoustics

Several methodologies have been developed to estimate wave characteristics for open sea and coastal studies. In both environments, the difficulties to obtain measurements also with rough sea increased the use of data provided by satellite and, in the meantime, gave rise to a growing interest in the autonomous system capable to measure meaningful parameters in a continuous way and in all meteo-marine conditions.

In-situ technologies such as wave buoys [12], pressure and acoustic water level sensors [13], and upward-looking acoustic Doppler current profilers (ADCPs) [14] are generally employed to monitor and estimate ocean waves. Nonetheless, the use of a wave buoy is quite prohibitive in real open ocean environment with sea bottom deeper than 1000 m. In this case, the only possibility to collect wave estimate on long-term basis is to employ vertically oriented sonar installed on spar buoys [15, 16] that do not follow the surface but are designed to allow for negligible sensitivity to sea heave and height.

Acoustic wave meter systems are commonly based on a directional array of high frequency precision, and acoustic altimeters are installed in an upward-looking configuration. The echosounder transmits a short pulse, and the acoustic returns are amplified and subjected to compensation through a time-varying-gain circuit, which corrects for acoustic losses associated with beam spreading and attenuation in sea water. After digitization, the amplitudes of the echo are scanned to select a single target for each ping. The selection procedure chooses the target with the longest persistence from all targets having amplitudes above a user-specified threshold level.

Under the hypothesis of a constant sound speed, each altimeter emits a single beam toward the sea surface and measures the time between the emission and the received echo. Under stationary conditions of the sea state, wave height process can be considered as a stationary and ergodic stochastic process with zero mean. However, a truthful statistical description of sea waves is achieved only if the wave height process is supposed to be Gaussian [17].

In a real environment, not all samples satisfy the properties of the Gaussian distribution, and the measured echoes of the array of altimeters could be disturbed by reverberation of bubbles, dishomogeneity close to sea surface, and the presence of fishes lying between the altimeter and the sea surface. To overcome these issues, an ad-hoc processing algorithm has taken into account the correction for the motion of the platform hosting the acoustic array.

## 2.3. Wave meter system on spar buoys

An acoustic wave meter system was installed at a depth of 10 m on the spar buoy part of the W1M3A observatory moored in the open Ligurian Sea (Northwestern Mediterranean Sea) [18].

The array was constituted of three brackets, which were 2.5 m long, equally spaced at  $120^\circ$ , hosting three high-frequency (500 kHz) altimeters that emit a narrow conical beam ( $6.0^\circ$  width at  $-3$  dB) which results in a small area being insonified at the surface (about 1.04 m). A Transistor-Transistor Logic (TTL) signal triggered the emission of the pulse by each altimeter. In order to avoid interferences, the acquisition system, which controlled and collected the

output signals from the altimeters, synchronized and slightly shifted in time with the three TTL signals so that each ping (and consequently each sample acquisition) was delayed with respect to the others of few milliseconds.

The slow motion of the spar buoy, especially in the presence of strong winds and currents, can influence the acoustic measurements, thus, the wave meter package was inclusive of vertical accelerometers and a couple of two axis orthogonal inclinometers installed along the horizontal axis to correct the acquired data for the buoy motion.

The acquisition system simultaneously collected the time series provided by the three echosounders at a frequency of 2 Hz and buoy motion data (inclination and acceleration). First, the time series of the three echosounders was quality controlled in order to identify spikes, outliers, and samples not satisfying the Gaussian condition. The detected samples were then interpolated by means of spline functions. In order to preserve the phase-shift information between the three time series in all the cases in which the reconstruction of part of the overall time series was not possible due to the elevated number of bad samples, all waveforms (provided by the altimeters, the inclinometer, and the accelerometer) were adjusted homogeneously.

The obtained time series was then filtered to compensate for platform motion [19], and standard statistical parameters (i.e., wave height, period) were computed on the basis of the spectral density features of the acoustic profiles [9, 20]. The wave meter system was designed to create an equilateral-triangular array (**Figure 1**), allowing the estimates of the prevalent direction of the wave by means of the theory of the direction of arrival [21] valid under the assumption of the incoming planar wave.

Let us consider to divide the three altimeters into pairs (i, j), (j, l), and (i, l): the time delay between the sensors of each pair when the planar wave passes through can be expressed in matrix form through Eq. (5):

$$\tau = \bar{X} \cdot \bar{k}. \quad (5)$$

$\tau, \bar{X}, \bar{k}$  represent the matrices of time delay, the displacement between the two devices of each pair, and the direction, respectively. If the triangularity condition between the three pairs (i, j), (j, l), and (i, l) of echosounder is satisfied ( $x_{(i,j)} + x_{(j,l)} + x_{(i,l)} = 0$ ), and it is known as the time delay vector, the propagation vector can be obtained by solving the least squares pseudo inverse Eq. (6).

$$\hat{k} = (X^T X)^{-1} X^T \hat{\tau}. \quad (6)$$

The assessment of the method was carried out comparing simultaneous wave estimates obtained by using the acoustic wave meter and acquired by a Datawell Waverider (DWR) directional buoy, a spherical one with 0.9 m of diameter, specifically designed to monitor wave characteristics. Wave data acquired by DWR buoys are basically displacement signals: one (the heave signal) for the non-directional wave rider and three (heave, north, and west displacement) for the directional wave rider. The mean, variance, skewness, and kurtosis of these signals are also computed. In the wave-statistical processing, zero-upcross waves are

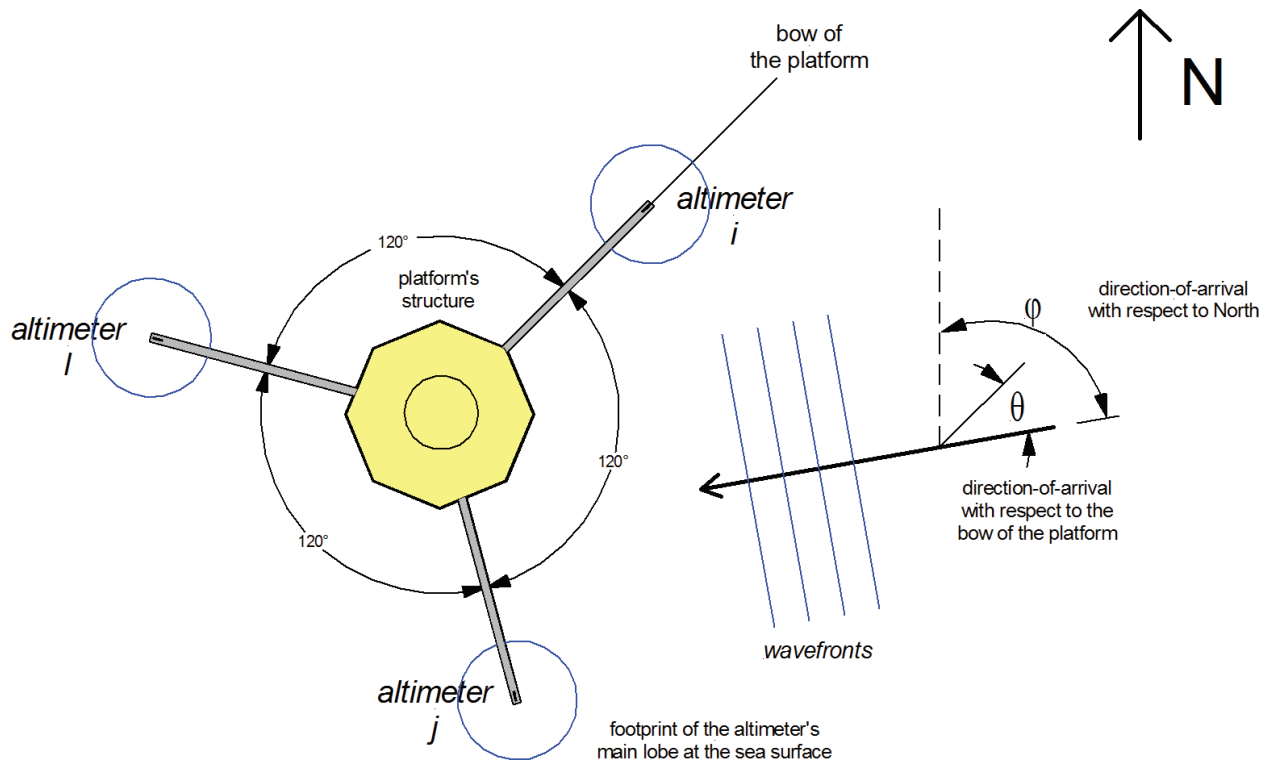


**Figure 1.** A sketch of the array of acoustic altimeters.

constructed from the heave signals, which are sorted by wave height and averaged in several fashions. This is the classic method of wave analysis that generates the significant wave height  $H_{1/3}$ . In the spectral analysis, the power spectral density is computed using Fourier methods. The wave direction as a function of wave frequency is calculated from the co-spectral and quadrature spectral densities of the three displacement signals. Using a maximum entropy method (MEM), the 3D spectrum, that is, the power spectral density as a function of both wave frequency and wave direction is computed.

The two buoys were moored at a nominal distance of 4 km for safety reasons, since the main buoy of the W1M3A observatory can span a circular area of 2 km by means of its slack mooring. These systems were continuously operational within the time of the validation which lasted 2 months from June to August, and all available estimates were used for the validation. During the period of the assessment, significant wave heights spanned from a minimum of 0.14 m to a maximum of 3.20 m and two storms occurred with the corresponding rough sea and strong wind speed. Thus, the acoustic wave meter was tested for several sea-state conditions. Although the majority of samples regard a smooth sea-state condition, a statistically significant number of samples refer to slight, and a moderate sea-state class was observed.

The validation of the acoustic wave meter system in terms of  $H_{1/3}$  was based on the slope and the intercept of the linear regression line, considering the estimates are obtained using the acoustic method as the independent variable and the DWR observations as the dependent variable. Due to the constraints of the designed array, only sea wave with period greater than 3.3 s could be successfully measured without aliasing issues. The performed analysis shows

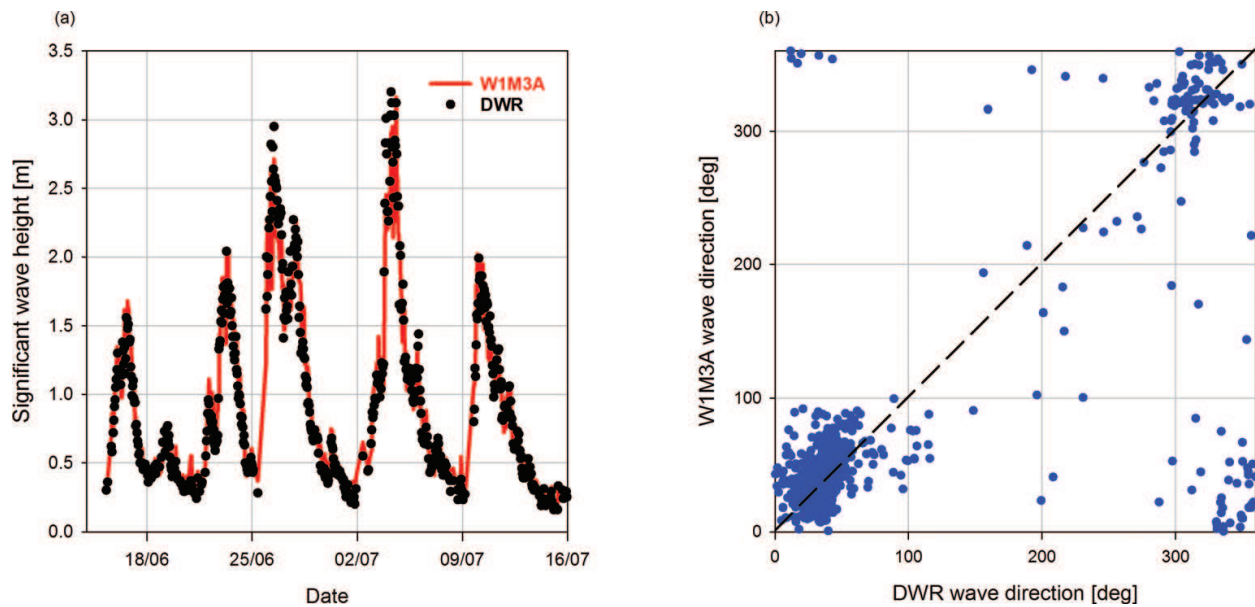


**Figure 2.** (a) Time series of significant wave height as estimated through the acoustic wave meter system and measured by the Datawell Waverider buoy. (b) Scatter plot of the wave direction estimated by the acoustic wave meter versus the one measured by the Datawell Waverider buoy.

a very good agreement between the two time series (**Figure 2a**) with a correlation coefficient of 0.97 and a linear regression defined by a slope of 0.9017 and an intercept of 0.1052. The observed small variations can be considered as a feature of the natural sea state since the measurements were carried out in two different positions, about two nautical miles far. Wave direction estimates were compared considering the results of the direction of the arrival technique for the W1M3A data and the most powerful direction retrieved by the DWR directional spectrum. Results show an overall satisfactory agreement within the error of  $\pm 15^\circ$  that is consistent with the accuracy of the DWR estimates, except for few cases related to changes in wind direction and low wind intensity (**Figure 2b**).

Results demonstrate the feasibility to use an acoustic wave meter array as an affordable tool to measure waves on the long term and also in an open ocean where it is difficult to deploy discus buoys on deep sea bottom for an extended period of time. The system is still deployed on the W1M3A observatory and the collected data were used to indirectly assess the performance of the Dust Regional Atmospheric Model (DREAM) model to predict sea salt aerosol concentrations [22].

### 3. Migratory patterns of zooplankton detected by acoustic Doppler current profiler

#### 3.1. Acoustic Doppler current profiler data

The first prototypes of acoustic Doppler current profilers were developed at the end of the 1980s with the aim of a continuous monitoring of ocean currents along the water column. Initially,

these instruments transmitted a single narrowband pulse and through the auto-correlation technique and provided measurements of the first spectral order. Ten years later, the second generation of ADCP was put on market. It was characterized by a wider band and an enhanced data processing, exploiting the principle of Doppler effects. Nowadays, ADCP instruments transmit a pulse with known frequency and listen to the return echo that is backscattered from water drop, sediments, planktonic organisms, and all particles that are freely transported by ocean currents.

Part of the transmitted sound is backscattered in all directions, part is dissolved in the ocean, and another part comes back to the instrument. This signal is twice phase shifted because of the Doppler effect: when the scattering elements present in the ocean move away from the transducer, the sound is phase shifted of a quantity proportional to their relative speed ( $S$ ) respect to the ADCP. If source and receiver are approaching or moving along a direction maintaining the same distance between them, no Doppler effect is present. For this reason, ADCP devices measure the parallel component to the acoustic beam, and the frequency of the signal turning back to the instrument ( $F_d$ ) can be described through Eq. (7).

$$F_d = 2F_p \left( \frac{S}{c} \right) \cos \alpha \quad (7)$$

$F_p$  is the frequency of the transmitted pulse,  $c$  is the sound speed in the ocean, and  $\alpha$  is the angles between the beam and the water speed.

Mathematically, a phase displacement corresponds to dilation in the time domain. The sound produced by a single particle and also its backscatter echo remains unchanged until the particle doesn't move, but in case of a small displacement from the source, the echo will need more time to reach the transducer and thus the return signal will be phase shifted. ADCP devices measure the phase of the signal to obtain the time dilation exploiting the principle that the speed of the particles can be calculated if the interval of time between two pulses is known. The only ambiguity is represented by the fact that the phase is measured in the interval  $0-360^\circ$  and when the phase exceeds  $360^\circ$ , it starts again at  $0^\circ$ . The easy solution consists of transmitting a train of pulses with very short time delay for each pulse in order to avoid changes in the phase of the particles of more than  $360^\circ$ .

Generally, ADCP instruments are constituted of two couples of transducers to measure north, east, and vertical components of the ocean current, and the profile is obtained subdividing the water column in several segments called bins. The main outputs of the ADCP devices are current speed and direction, but several ancillary parameters, used to calculate current characteristics, are also available.

### 3.2. Diel vertical migration of zooplankton

The diel vertical migration (DVM) can be defined as the cyclic vertical displacement performed by most zooplankton species. Different DVM patterns have been observed, but the most common behavior is the swimming upward at sunset and downward at sunrise. Several environment causes such as light, temperature, food, and predation pressure, as well as

endogenous origins like sex and age, influence DVM characteristics. Generally, the vertical distribution of the zooplankton is determined by net tows or pump samples that allow one to identify with the different species, but these samples are sparse in time and space and do not provide detailed information on the temporal variability, especially in the long-term period.

ADCP instruments are a powerful tool to overcome this issue, guaranteeing a quite continuous monitoring, also in extreme environments such as the Polar regions [23, 24] or highly productive basin, such as the Mediterranean Sea [25–27], at the expense of a specific taxonomic analysis.

Patterns of DVM can be detected through the analysis of the backscatter strength data ( $S_v$ ) of the signal that, for the current profiler made by [28], can be expressed by Eq. (8).

$$S_v = 20 \log R + 2\alpha R - A + 10 \log \left( 10^{\frac{KE}{10}} - 10^{\frac{KE_r}{10}} \right)$$

$$K_c = \frac{127.3}{T_x + 273}$$

$$R = \frac{B + \left( \frac{L+D+L_a}{2} \right) + [(n-1)D] + \frac{D}{4}}{\cos \vartheta}$$
(8)

$\alpha$  is the absorption coefficient,  $T_x$  is the internal temperature of the device in °C,  $B$  is the distance in m beyond which the measure is valid,  $L$  is the length in m of the transmitted pulse,  $D$  is the dimension in m of the bin,  $L_a$  is the lag length of the pulses in m,  $n$  is the number of the cell in which the measure is taken, and  $\vartheta$  is the inclination angle of the transducers.  $E$  is the raw echo signal as measured by the ADCP and  $E_r$  is the minimum acquired value during the deployment.  $R$  is defined as slant range and represents the spatial coefficient related to the inclination of the pulses with respect to the vertical of the instrument. The constant  $A$  is the best linear regression fit between Eqs. (8) and (9) proposed in Ref. [29] for all samples satisfying the condition of signal-to-noise ratio exceeding 10 ( $K_c(E-E_r) < 10$ ).

$$S_v = C + 10 \log \left( (T_x + 273.16) R^2 \right) - L_{DBM} - P_{DBM} + 2\alpha R + K_c (E - E_r)$$

$$R = \frac{B + \left( \frac{L+D}{2} \right) + [(n-1)D] + \frac{D}{4}}{\cos \vartheta} \left( \frac{C'}{C_1} \right)$$
(9)

$C$  is a constant typical for each model of Teledyne RD Instruments (RDI) profiler and  $L_{DBM}$  and  $P_{DBM}$  are the logarithms of pulse length in m and of power transmission in Watt, respectively.  $C'$  is the sound velocity depending on the depth and  $C_1$  is the sound speed used by the instrument to calculate the time between the pulse transmission and the received echo.

Equation (8) was applied to high-resolution acoustic ADCP backscatter data acquired during winter 2009–2010 in the Ligurian Sea. The used backscatter data were provided by an upward looking 300 kHz ADCP (by RDI) deployed at about 150 m depth on a deep sea bed of 1200 m from November 2009 to April 2010. The device was set to sample every 15 min with a bin length of 2 m in order to obtain high resolution data both in time and in space.

Backscatter strength values show a seasonal variability with low values in winter from 70 m depth down to 127 m and a gradual increase till 100 m in early spring in correspondence with

the increment of the net primary productivity that, in turn, implies more availability of food in the water column and less need for the zooplankton population to reach the surface to feed themselves. The analysis of the  $S_v$  time series clearly evidences a circadian cycle with a quite perfect agreement between the decrease of backscatter intensity and the hour of sunrise (spanning from 5:08 to 06:38 UTC in the deployment period) and, vice versa, an increase of  $S_v$  in correspondence to the hours of sunset (ranging from 15:48 to 17:50 during the deployment). The analysis of corresponding vertical speed presents negative values around dusk and positive ones at dawn, showing a well-defined nocturnal DVM pattern with a rapid ascent of zooplankton from the bottom to the sea surface during dusk and a rapid descent from the surface to deep water at dawn (Figure 3).

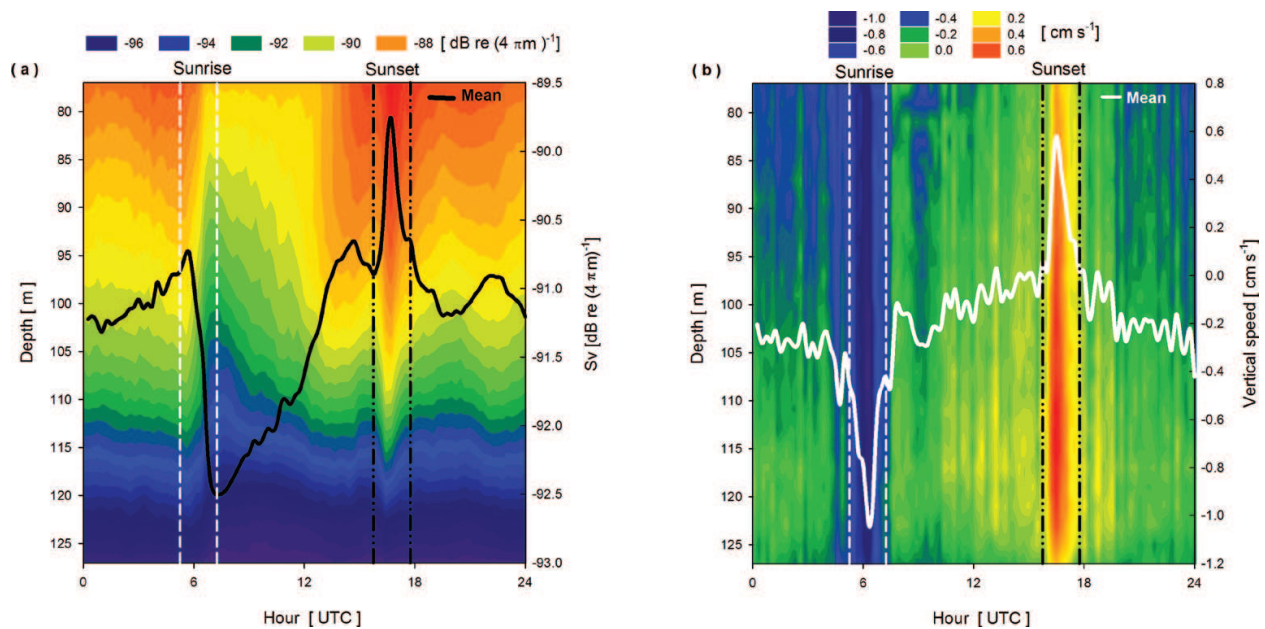


**Figure 3.** (a) Daily averaged backscatter strength with, superimposed, the mean values and (b) daily averaged vertical velocity with, superimposed, the mean values, the hours of sunrise and sunset.

Furthermore, in December and January, the DVM was influenced by moonlight: during full moon nights and clear skies (December 2 and 31, 2009), the backscatter strength decreased in the surface layers while greater values extended in the water column down to the maximum analyzed depth, making the values acquired at different depths quite homogenous along the water column (Figures 4a and b). This behavior, in contrast with the common nocturnal DVM of new moon periods (Figures 4c and d), is a characteristic of macrozooplankton/micronekton species and can be interpreted as a way to escape from visual predators [30]. Indeed, corresponding vertical velocities show more variability in the surface layers and a marked downward movement at midnight that is not present during the other moon phases (Figures 4e and f).

Obtained results demonstrate the feasibility to use non-calibrated ADCP data to infer zooplankton behavior with respect to daily seasonal and inter-annual variability as well as to astronomic phenomena. In fact, the observed intense DVM signal can be an indication of the presence of the *Clausocalanus* spp., *Fritillaria* spp., and, among the macrozooplanktons/

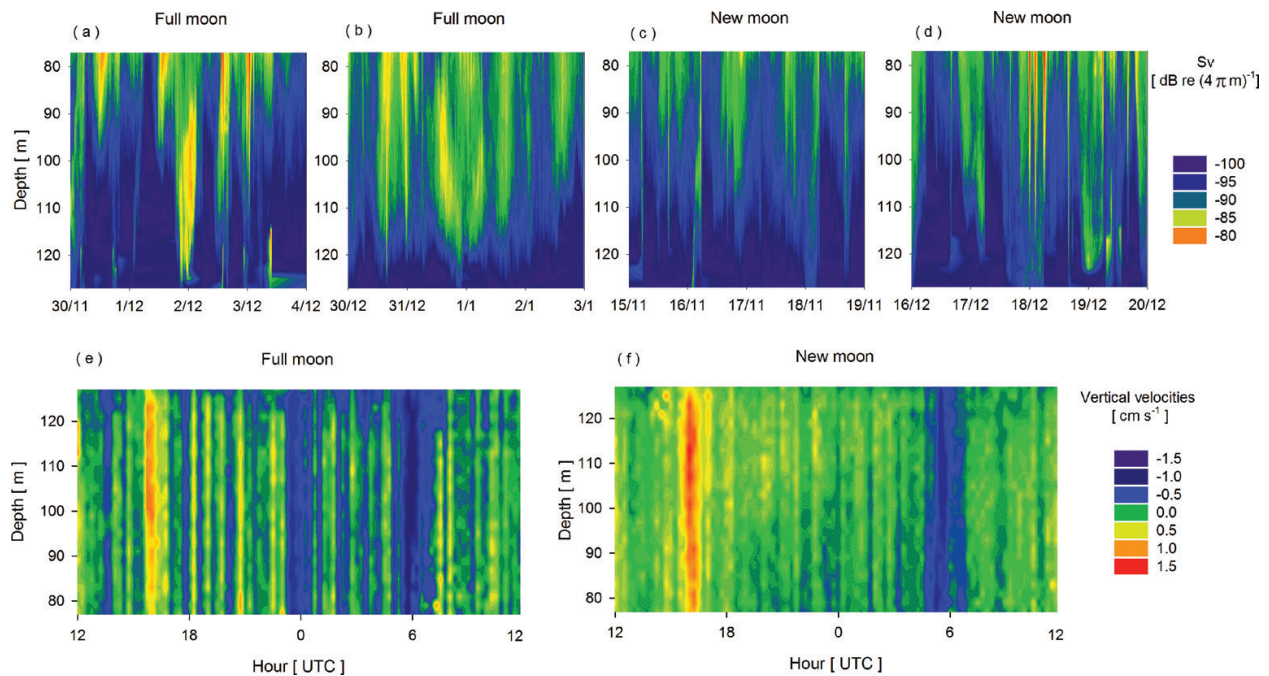


**Figure 4.** Temporal series of backscatter strength profiles during the full moon on (a) 2, December 2009 and (b) 31, December 2009 and (e) the corresponding average vertical velocities. Temporal series of backscatter strength profiles during the new moon on (c) 16, November 2009 and (d) 16, December 2009 and (f) the corresponding average of vertical velocities.

micronektons, of euphausiids (mainly *Meganyctiphanes norvegica*) that perform nocturnal migration and are abundant in the Ligurian Sea from December to March. Furthermore, the different patterns of DVM seen during full moon nights further support the hypothesis of the presence of euphausiids since, among the main migrators in the Ligurian basin, only euphausiids exhibit a sinking closely related to moonrise.

## 4. Ocean monitoring through passive acoustic measurements

### 4.1. Ocean environmental noise

Within the framework of the “Marine Strategy Directive to save Europe’s seas and oceans” edited in June 2008, one of the main challenges of the Europe member state is to adopt mitigation actions and policy plans aiming at an effective protection of the overall marine environment by 2020. The increase of the maritime traffic and of anthropogenic activities at sea, such as the extensive use of sonar and oil drilling activities, has contributed to modify the natural ocean environmental noise so much that in some basins, it is the main cause of changes in the behavior of marine mammals.

Underwater environmental noise plays a fundamental role in biodiversity conservation, and the first studies date back to the Second World War when acoustic experiments established that environmental noise is the sum of several factors including ship traffic, breaking waves, wind, rain, mammals’ vocalizations, and sound produced by marine organisms. In 1962,

Wenz [31] demonstrated that ships generate noise at low frequencies and proposed curves that describe the spectrum level at different frequencies for noise generated by ships and wind that were at the base, and still are, of forecasting systems. The National Research Council in Ref. [32] introduced a new definition of environmental noise as the “*noise associated with the background din emanating from a myriad of unidentified sources.*” The most common sources can be distinguished by their acoustic signatures and can be subdivided into four major groups depending on their origin: physical, geological, biologic, and anthropogenic.

Wind is the major physical producer of noise over sea surface, and its spectral characteristics span a broadband frequency band, from less than 1 up to 50 kHz. The spectral curves show an increment for frequencies below 1 Hz, followed by a decrease as frequencies increase. As wind speed increases, the spectral curves maintain the same shape but show greater pressure levels. For wind speed  $> 10 \text{ ms}^{-1}$ , the sound produced on the sea surface can be undistinguished by the sound due to the passage of a distant ship. Moreover, it is often associated with a high wave that is responsible for the generation of small bubbles that, in turn, produce sound and make the detection, and especially the quantification, quite difficult.

Also, precipitation contributes to the ocean noise in the frequency band from hundreds of Hz to more than 20 kHz, and the corresponding spectra show different characteristics depending on the type of precipitation. In the case of drizzle, a clear peak originated at the acoustic resonance of small drops splashing on the sea surface is observable around 15 kHz. This peak tends to disappear with the increase of the drops' dimension that produce sound at a frequency lower than 10 kHz and another peak at about 1–2 kHz in case of convective rain.

Tectonic processes, earthquakes, volcanic, and hydrothermal activities are the major geological sources contributing to the ocean environmental noise. Their spectra range from 1 to 100 Hz, show an initial burst, and the same noise persists for several minutes.

Biological sources are strictly related to marine organisms and mammals living in the ocean that produce signals spanning from 10 up to 200 kHz, depending on the species. In very productive basins, the biological sources are prevalent on the physical and geological components, whereas in high anthropological areas, the main responsible events of the noise are human activities.

Noise generated by ship passages is characterized by low frequencies (5–500 Hz) and propagates over long distances affecting wide areas. Each type of vessel (research vessels, leisure or fishing boats, tankers, commercial ferries, etc.) and also each single vessel are characterized by an own acoustic signature depending on cavitation phenomena, on the modulation of blade propeller, and on the on-board engines. Furthermore, noise produced by ships is variable and could be affected by environmental conditions especially for the interaction with the sea bottom.

Measurements of ocean environmental noise are related to the power of the propagating signal and to the characteristics of the acoustic path between source and receiver that can be modified by oceanographic dynamics, sound velocity propagation, and bathymetry. These components cause fluctuations in the pressure levels of the environmental noise depending on depth, time instants, and areas; thus, it is necessary to perform further experiments and to

continuously monitor environmental noise to deepen the knowledge of its dynamic and the impact of the human activities.

#### 4.2. Rainfall and wind speed measurements inferred by acoustic passive measurements

Passive acoustic data of ocean ambient noise consists of measurements of sound pressure as a result of the superimposition of sounds generated by several types of events (i.e., rainfall, ship passages, or mammals' vocalizations) to background noise, which is the natural noise in the absence of any sources, whose level is closely related to the intensity of blowing wind. Although background noise levels can be different from basin to basin, each source shows unique spectral characteristics that can be used to classify its type (physical, biological, anthropogenic) and, in some cases, also to obtain an estimate of atmospheric parameters over the sea surface (i.e., wind, rain). Indeed, multivariate analysis techniques can be applied to a combination of spectral levels, acquired at specific frequencies and least-square fit in different spectral bands to provide insights about the different sources forming the environmental noise.

**Figure 5** shows the results of the multivariate analysis applied to acoustic data that was acquired in the open Ligurian Sea from March to November 2015 by means of a hydrophone installed on the W1M3A observatory. The output signal of the hydrophone was band-pass filtered and then digitalized at 16 bit with a sampling frequency of 100 kHz. Acoustic data

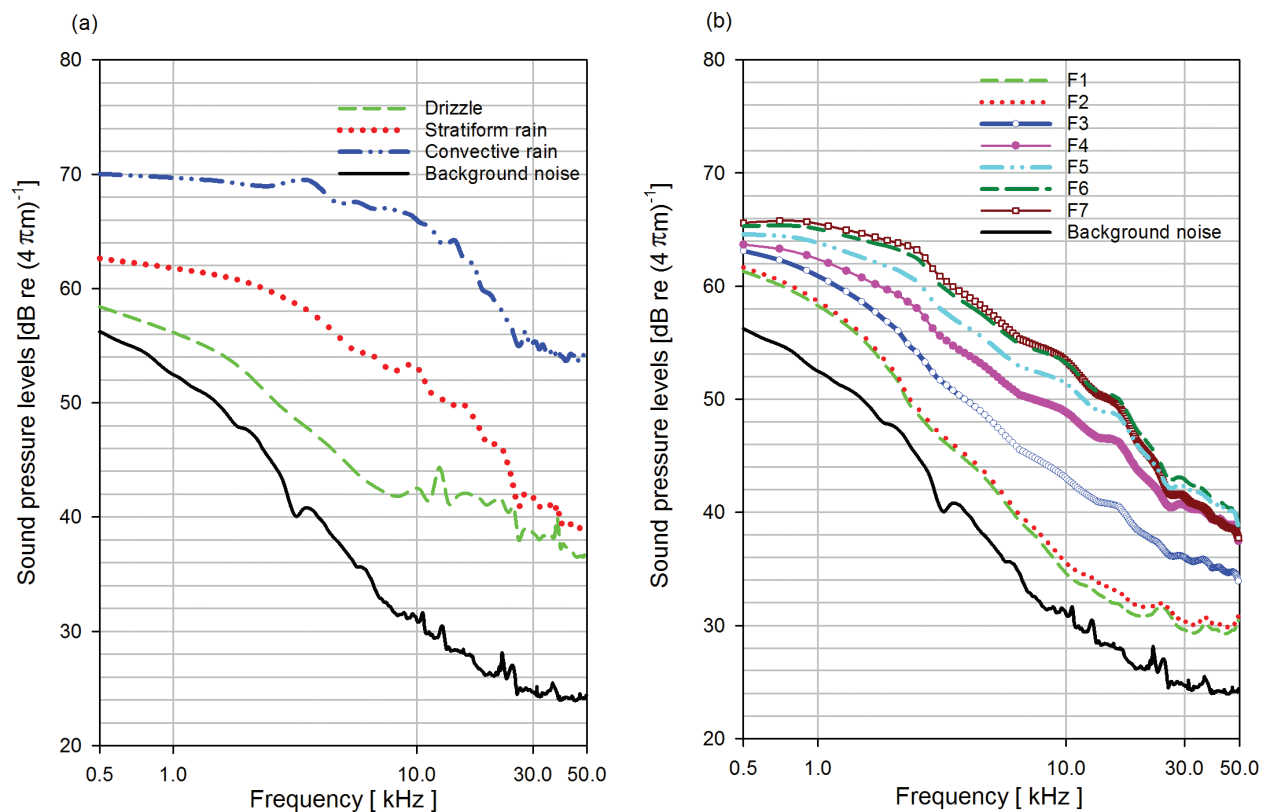


**Figure 5.** Average sound spectra for (a) different types of precipitation and (b) wind speed greater than 2 ms<sup>-1</sup> subdivided in Beaufort classes compared to the average spectrum of the background noise.

were collected for few seconds, every tens of minutes, due to the large amount of data that such a sampling rate produces.

During the analyzed period, wind was continuously blowing over the sea surface and generated a sound that increased proportionally to the reinforcement of its speed, and, similarly, spectral levels tended to increase monotonically from 0.5 to about 25 kHz. Beyond this threshold, the sound produced by strong wind resulted comparable and even lower than the one generated by moderate breeze because of the contemporary arising of large waves and, in turn, the generation of small bubbles that absorbed the emitted sound. Wind spectra were very different to the one obtained during episodes of convective rain but could mask events of stratiform and light rain since the spectral levels from 20 up to 30 kHz were very similar for wind speed greater than  $8 \text{ ms}^{-1}$ . Furthermore, the resonance frequency of bubbles splashing on the sea surface is inversely proportional to their size and for this reason, large drops associated with heavy rain showed loud sound and, instead, small drops, typical of light rain events, presented a peak in the 10–15 kHz frequency band.

Several studies were carried out to quantify wind speed and rainfall amounts through the analysis of acoustic data. In Ref. [33], a logarithmic relation based on the sound pressure levels acquired at 8 kHz was proposed, and, recently, new parameterizations has been introduced for the Mediterranean region based on the results achieved during the Ionian Sea rainfall experiment and Ligurian sea acoustic experiment [34, 35].

The equation proposed in Ref. [35] was applied to the acquired acoustic data and compared to the in-situ wind speed observations provided by the W1M3A observatory for wind speed greater than  $2 \text{ ms}^{-1}$  (**Figure 6a**). Results show a good agreement between wind speed measurements provided by the anemometer and the estimates obtained using acoustic data, with a correlation of 87.5% and a root mean square error of  $1.294 \text{ ms}^{-1}$  taking into account that  $2 \text{ ms}^{-1}$  can be considered as the minimum wind speed that is acoustically detectable.

Rainfall rate and sound intensity are related by a logarithmic expression based on the sound pressure level at 5 kHz, whose coefficients can vary depending on the area of deployment [36]. Available acoustic data acquired in 2015 were processed following the algorithm proposed in Ref. [35] and compared to rainfall observations simultaneously acquired by a rain gauge installed on the W1M3A offshore observing system (**Figure 6b**). Results evidence the feasibility to use passive acoustic data to detect rainfall episodes, especially in case of intense events and the capability of quantity rainfall amounts with good accuracy, independently from rain types and the presence of wind speed.

#### **4.3. Marine mammals monitoring through passive acoustic observations**

Passive acoustic observations provide powerful support to complement visual surveys for the monitoring of marine mammals due to the fact that acoustic waves propagate for long distance. Visual observations are weather dependent, not available in remote or inaccessible areas, often limited in their use due to the short times animals may spend at the surface, and are sparse in time, whereas passive acoustic devices can be successfully employed for an extended period of time and can monitor a wide area providing information about both the presence and the species of the animals.

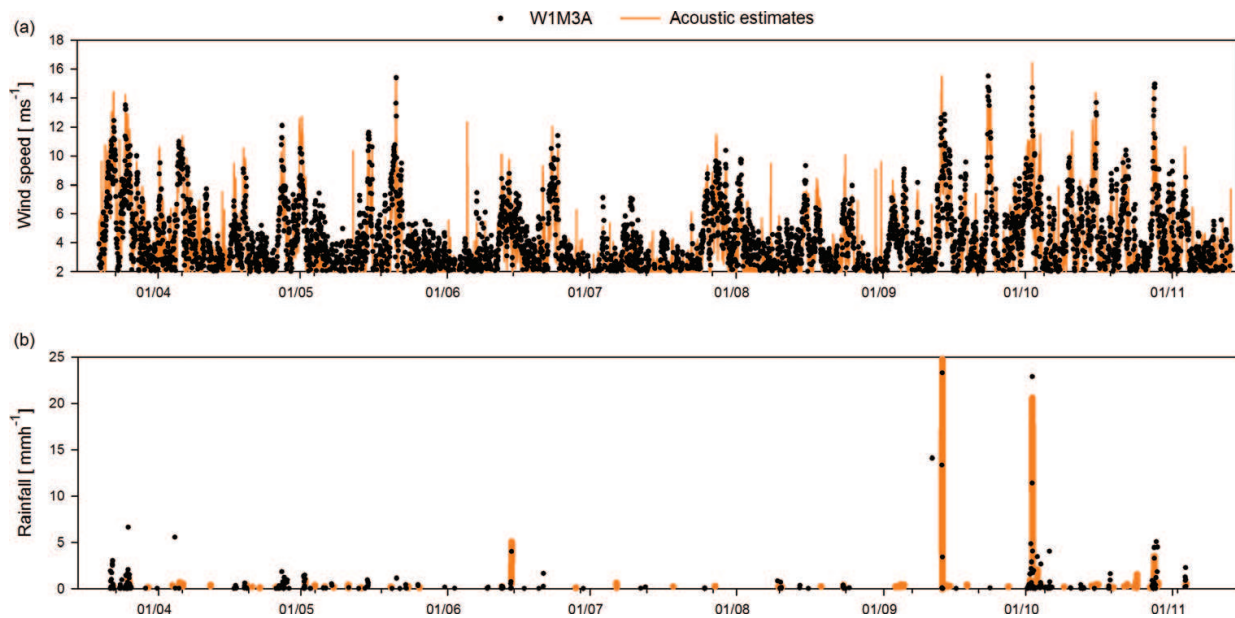


**Figure 6.** Time series of (a) wind speed and (b) rainfall as measured by the anemometer and the rain-gauge installed on the W1M3A marine observatory, and the estimates obtained from acoustic samples.

Vocalizations are the principal sounds generated by marine mammals that use them to communicate, to echolocate, and also for predatory or mating purposes [37]. Every species, and even each individual, can be recognized by its acoustic signatures, and for this reason, time-frequency analysis of time series of passive acoustic data is useful for the marine mammals' monitoring. This is particularly true for basins where human activities are scarce and the environmental noise is dominated by mammals' vocalizations like Thetys Bay in Antarctica or in a very productive area such as the “Cetacean Sanctuary” in the Ligurian Sea.

During the 29th Italian Antarctic expedition, a hydrophone was installed under the sea ice in Thetys Bay to study sound propagation. The basin is a natural habitat of different pinnipeds species (i.e., crabeater seal (*Lobodon carcinophaga*), leopard seal (*Hydrurga leptonyx*), Ross seal (*Ommatophoca rossii*), and Weddel seal (*Leptonychotes weddellii*)), and the vocalizations of some of these mammals were the preponderant sound in the collected measurements (**Figure 7**).

The experiment took place in November, during the Weddel seals mating period [38], and this explains the reason why the prevalent types of detected calls from Weddel seals are trills and whistles, both ascending or descending as defined in Ref. [39]. Trill calls show a descending pattern, are emitted once, last for 15 s and cover a wide frequency range from 6 kHz down to few hundreds of Hz. Whistles ascending, although being single pulses, last few seconds maximum, and their patterns are characterized by a sharp increase from about 4 up to 5 kHz, followed by a smooth rise up to 6 kHz maximum. Whistles descending are a series of pulses initially emitted at about 1-s intervals, progressively reducing the interval and dropping from 10 to 2 kHz. The typical vocalization produced by crabeater seal is known as moan; its spectrum has power content lower than trills and whistles in the whole range of frequencies and the signal spans from 700 up to 6 kHz.

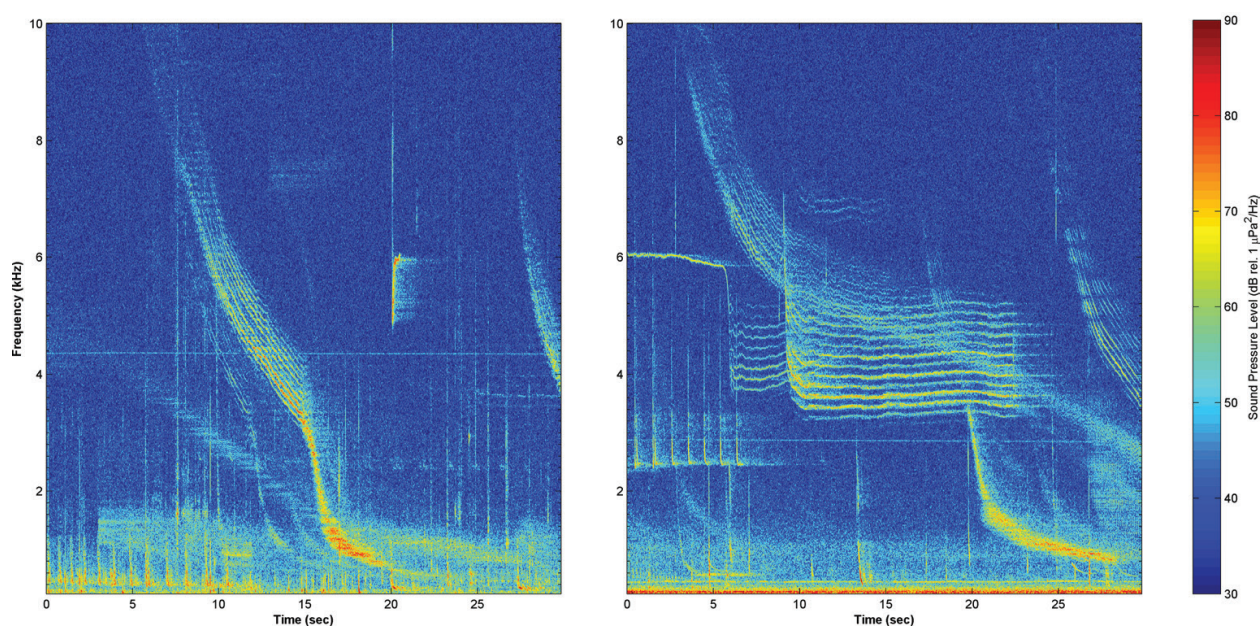


**Figure 7.** Spectrograms of vocalizations by Weddell and crabeater seals acquired during the 29th Italian Antarctic expedition.

A similar experiment took place in the Ligurian Sea during 2015, allowing one to identify the presence of sperm whales (*Physeter macrocephalus*), striped dolphins (*Stenella coeruleoalba*), and Cuvier's beaked whales (*Ziphius cavirostris*) through the analysis of their spectrograms (**Figure 8**).

Sperm whales are the most common mysticete species in the Ligurian-Corsican-Provençal basin due to the high productivity that characterized the area supported by the permanent frontal structure of rich large biomass of krill, especially of *Meganyctiphanes norvegica* that is the favorite prey of the sperm whales. The vocalizations of sperm whale are constituted of sequences of clicks, which are brief impulsive sounds, variable in length that can reach 35 kHz in frequency. The pattern is depending on the area, the sex, the age of the animal, and also on the meaning: train of pulses with a repetition rate of two to three clicks per second are emitted during the diving to make recognition of the environment or for hunting, whereas high rate clicks referable to creaks are commonly used for echolocation.

Odontocetes calls are much different from mysticete's vocalization, presenting a wide variety of patterns of whistles ranging from few Hz up to more than 20 kHz and clicks used for echolocation that can extend between 50 and 150 kHz. Using the spectrograms, it is possible to distinguish the different species of the odontocetes and, in some cases, the sound emitted by the same individual.

The availability of passive acoustic recordings covering a long period of time could really improve the knowledge of mammals' vocalizations in their natural environment, especially in winter months where it is difficult to carry out visual surveys due to potential bad weather conditions.

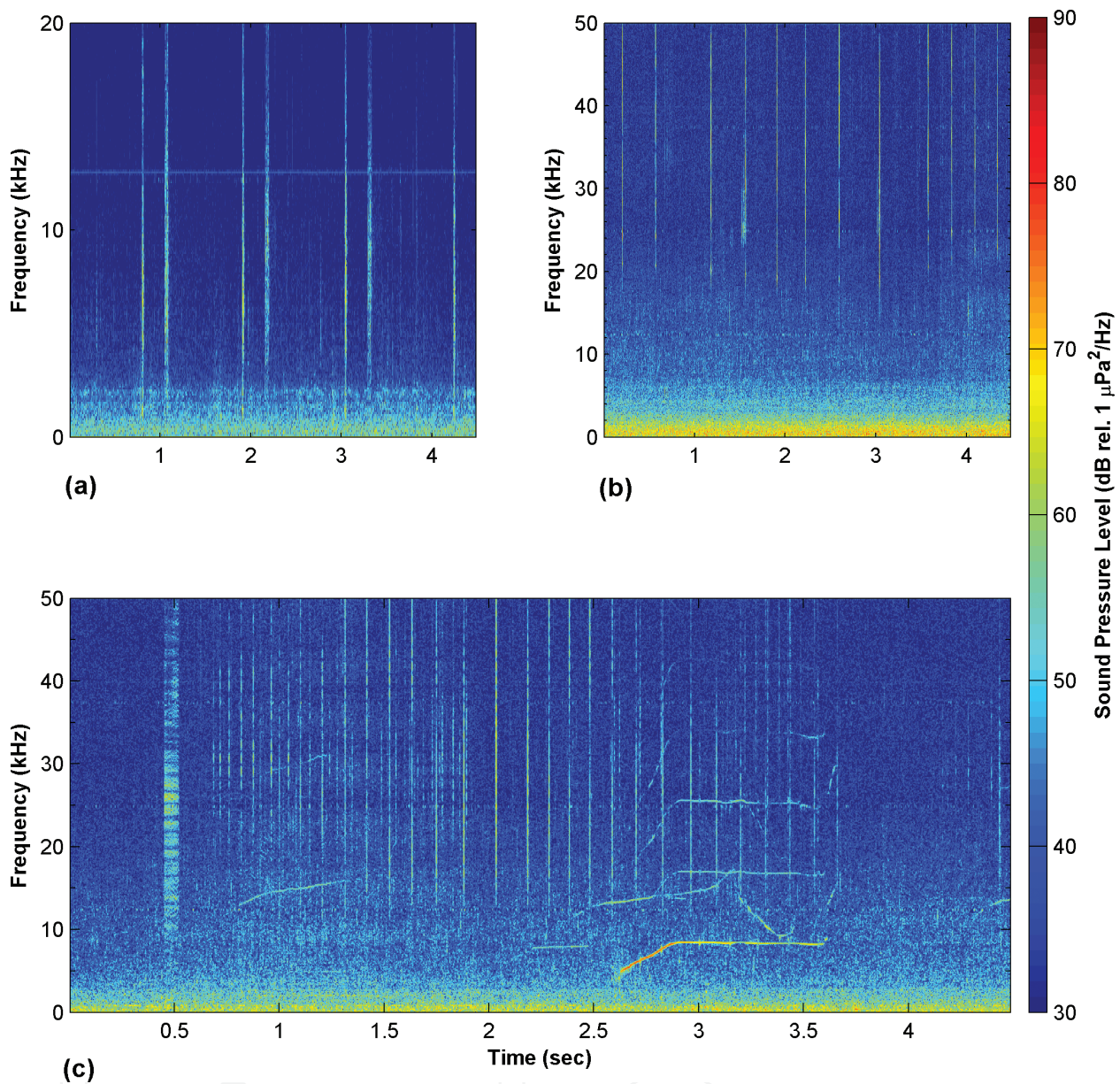


**Figure 8.** Spectrograms of vocalization by (a) sperm whales, (b) Cuvier's beaked whales, and (c) striped dolphins acquired in the Ligurian Sea.

## 5. Summary

The combination of active and passive underwater acoustic methods could significantly contribute to the monitoring of the oceanic environment and to a better characterization of the ocean status. Analysis of acoustic observations in the time domain allows the detection of seasonal trends or inter-annual variability helpful for the identification of climate change's causes and/or impacts, as well as for the definition of mitigation actions and strategic plans devoted to the protection of the marine environment. Otherwise, analysis of acoustic data in the frequency domain makes possible to distinguish geophysical phenomena, such as wind and rain, and biological sources, such as vocalizations of marine mammals and anthropogenic

noise by means of their own acoustic signatures. Specifically, the application of Fast Fourier Transform (FFT), wavelet, and autocorrelation techniques could provide insights about wave fields and give evidence of the presence of several marine mammals or different patterns referable to migratory processes, typical of zooplankton and micronekton species.

Indeed, in-situ acoustic measurements provided by a directional array of upward looking echosounders, installed on a spar buoy, have been used to obtain estimates of wave height, period, and direction in the open Ligurian Sea. Results show the feasibility to use acoustics to obtain reliable observations of wave field using a fixed platform not specifically designed to follow the slope of the waves. Measurements provided by active devices have been also successfully employed to monitor the behavior of zooplankton in relation to daily cycle and moon illumination for a long period of time that cannot be obtained using sporadic cruises or net samples sparse in time.

Experiments based on the installation of hydrophones carried out in different basins demonstrated the potentiality of passive acoustic data used to identify a variety of processes. Known as the mean noise level of the basin in which the hydrophones are deployed, it was possible to apply algorithms to automatically quantify rain and wind by means of the noise produced on the sea surface. Furthermore, the application of time-frequency analysis allowed the creation of spectrograms from which the types of mammals living in a different basin were easily detected.

## Acknowledgements

The research leading to these results has received part of the funding from the European Community's Seventh Framework Programme FP7/2007–2013 under the grant agreement n° 312463 (FixO3) and the Flagship Project RITMARE funded by the Italian Ministry of Education, University, and Research.

## Author details

Sara Pensieri\* and Roberto Bozzano

\*Address all correspondence to: [sara.pensieri@ge.issia.cnr.it](mailto:sara.pensieri@ge.issia.cnr.it)

Institute of Studies on Intelligent Systems, National Research Council of Italy, Genova, Italy

## References

- [1] Zampoukas N, Piha H, Bigagli E, Hoepffner N, Hanke G, Cardoso AC. Monitoring for the Marine Strategy Framework Directive: Requirements and Options. European Commission—Joint Research Centre, Institute for Environment and Sustainability, Luxembourg; 2012. DOI: 10.2788/77640

- [2] Sund O. Echo sounding in Fisheries Research. *Nature*. 1956;**135** p.593. doi:10.1038/135953a0
- [3] Urick RJ. Principles of Underwater Sound. 3rd ed. New York: McGraw-Hill, Inc.; 1983. p. 423
- [4] Wall Bell CC, Rountree RA, Juanes F. Mapping the acoustic soundscape off Vancouver Island using the NEPTUNE Canada Ocean Observatory. *Advances in Experimental Medicine and Biology*. 2016;**875** p. 1205-1211, doi: 10.1007/978-1-4939-2981-8\_151
- [5] Erbe C, Verma A, McCauley R, Gavrilov A, Parnum I. The marine soundscape of the Perth Canyon. *Progress in Oceanography Part A*. 2015;**137**:38-51. DOI: 10.1016/j.pocean.2015.05.015
- [6] Adam O, Glotin H. Passive acoustic storey of the Antares neutrino detector for real-time cetaceans detection, localization and behavior studies. In: *New Trends for Environmental Monitoring Using Passive Systems*; Institute of Electrical and Electronics Engineers (IEEE), Hyeres, French Riviera. 2008. pp. 1-6. DOI: 10.1109/PASSIVE.2008.4786981
- [7] André M, van der Schaar M, Zaugg S, Houégnigan L, Sánchez AM, Castell JV. Listening to the deep: Live monitoring of ocean noise and cetacean acoustic signals. *Marine Pollution Bulletin*. 2011;**63**(1-4):18-26. DOI: 10.1016/j.marpolbul.2011.04.038
- [8] Tasker ML, Amundin M, André M, Hawkins A, Lang W, Merck T, Scholik-Schlomer A, Teilmann J, Thomsen F, Werner S, Zakharia M. Marine Strategy Framework Directive—Task Group 11 Underwater noise and other forms of energy. EUR—Scientific and Technical Research Series ed. Joint Research Luxembourg, Centre; 2010. p. 55. DOI: 10.2788/87079
- [9] Earle MD, Bishop JM. *A Practical Guide to Ocean Wave Measurement and Analysis*. Marion: Endeco Inc.; 1984
- [10] Massel SR. *Ocean Surface Waves; their Physics and Prediction*. London: World Scientific Publication; 1996
- [11] Holthuijsen LH. *Waves in Oceanic and Coastal Waters*. Cambridge: Cambridge University Press; 2007. p. 387
- [12] Varstow SF, Ueland G, Krogstad HE, Fossum BA. The Wavescan second generation directional wave buoy. *IEEE Journal of Oceanic Engineering*. 1991;**16**(3):254-266
- [13] Weiergang J. Wave measurement by single beam acoustic profiling. In: *Proceedings of the ECUA 1992; 14-18 September*: Elsevier Applied Science; Luxembourg. 1992. pp. 157-160
- [14] Terray EA, Grodon RL, Brumley B. Measuring wave height and direction using upward-looking ADCPs. In: *Proceedings of the IEEE OCEANS '97; 6-9 October*; Halifax. 1997
- [15] Graber HC, Terray EA, Donelan MA, Drennan WM, Van Leer JC, Peters DB. ASIS—a new Air–Sea Interaction Spar buoy: Design and performance at sea. *Journal of Atmospheric and Oceanic Technology*. 2000;**17**:708-720

- [16] Zedel L. Deep ocean wave measurements using a vertically oriented sonar. *Journal of Atmospheric and Oceanic Technology*. 1994;**11**:182-191
- [17] Rychlik I, Johannesson P, Leadbetter MR. Modelling and statistical analysis of ocean-wave data using transformed Gaussian processes. *Marine Structures*. 1997;**10**:13-47
- [18] Canepa E, Pensieri S, Bozzano R, Faimali M, Traverso P, Cavaleri L. The ODAS Italia 1 buoy: More than forty years of activity in the Ligurian Sea. *Progress in Oceanography*. 2015;**135**:48-63. DOI: 10.1016/j.pocean.2015.04.005
- [19] Anctil F, Donelan MA, Drennan WM, Graber HC. Eddy correlation measurements of air-sea fluxes from a discus buoy. *Journal of Atmospheric and Oceanic Technology*. 1994;**11**:1144-1150
- [20] Rychlik I. A note on significant wave height. *Oceanic Engineering*. 1996;**23**(6):447-454
- [21] Pirinen TW, Yli-Hietanen J. Time delay based failure-robust direction of arrival estimation. In: 2004 Sensor Array and Multichannel Signal Processing Workshop Proceedings; Institute of Electrical and Electronics Engineers (IEEE), Barcelona, 2004. pp. 618-622. DOI: 10.1109/SAM.2004.1503023
- [22] Kishcha P, Starobinets B, Bozzano R, Pensieri S, Canepa E, Nickovic S, di Sarra A, Udisti R, Becagli S, Alpert P. Sea-salt aerosol forecasts compared with wave height and sea-salt measurements in the open sea. In: Down GS, Trini Castelli S, editors. *Air Pollution Modeling and its Applications XXI*. NATO Science for Peace and Security Series-C: Environmental Security. Dordrecht, Springer; 2012. pp. 299-303. DOI: 10.1007/978-94-007-1359-8\_51
- [23] Cisewski B, Strass VH, Rhein M, Krägefsky S. Seasonal variation of diel vertical migration of zooplankton from ADCP backscatter time series data in the Lazarev Sea, Antarctica. *Deep-Sea Research Part I: Oceanographic Research Papers*. 2010;**57**(1):78-94. DOI: 10.1016/j.dsr.2009.10.005
- [24] Picco P, Schiano ME, Pensieri S, Bozzano R. Time-frequency analysis of migrating zooplankton in the Terra Nova Bay polynya (Ross Sea, Antarctica). *Journal of Marine Systems*. 2017;**166**:172-183. DOI: 10.1016/j.jmarsys.2016.07.010
- [25] van Haren H. Internal wave-zooplankton interactions in the Alboran Sea (W-Mediterranean). *Journal of Plankton Research*. 2014;**36**(4):1124-1134. DOI: 10.1093/plankt/fbu031
- [26] Bozzano R, Fanelli E, Pensieri S, Picco P, Schiano ME. Temporal variations of zooplankton biomass in the Ligurian Sea inferred from long time series of ADCP data. *Ocean Science*. 2014;**10**:93-105. DOI: 10.5194/os-10-93-2014
- [27] Pinot J, Jansá J. Time variability of acoustic backscatter from zooplankton in the Ibiza Channel (Western Mediterranean). *Deep Sea Research Part I*. 2001;**48**:1651-1670
- [28] Gostiaux L, Van Haren H. Extracting meaningful information from uncalibrated back-scattered echo intensity data. *Journal of Atmospheric and Oceanic Technology*. 2010;**27**(5):943-949

- [29] Deines L. Backscatter estimation using broadband acoustic Doppler current profilers. In: Oceans 99 MTS/IEEE Conference Proceedings; 13-16 September 1999; Institute of Electrical and Electronics Engineers (IEEE), San Diego, CA, USA
- [30] Tarling GA, Buchholz F, Matthews JBL. The effect of a lunar eclipse on the vertical migration behaviour of *Meganyctiphanes norvegica* (Crustacea: Euphausiacea) in the Ligurian Sea. *Journal of Plankton Research*. 1999;**21**(8):1475-1488
- [31] Wenz GM. Acoustic ambient noise in the ocean: Spectra and sources. *Journal of the Acoustical Society of America*. 1962;**34**:1936-1956
- [32] National Research Council, editor. *Ocean Noise and Marine Mammals*. National Academies Press; Washington, D.C. 2003
- [33] Vagle S, Large WG, Farmer DM. An evaluation of the WOTAN technique of inferring oceanic winds from underwater ambient sound. *Journal of Atmospheric and Oceanic Technology*. 1990;**7**:576-595. DOI: 10.1175/1520-0426(1990)007<0576:aeotwt>2.0.co;2
- [34] Anagnostou MN, Nystuen JA, Anagnostou EN, Nikolopoulos EI, Amitai E. Evaluation of underwater rainfall measurements during the Ionian Sea rainfall experiment. *IEEE Transactions on Geoscience and Remote Sensing*. 2008;**46**(10):2936-2946. DOI: 10.1109/tgrs.2008.2000756
- [35] Pensieri S, Bozzano R, Nystuen JA, Anagnostou EN, Anagnostou MN, Bechini R. Underwater acoustic measurements to estimate wind and rainfall in the Mediterranean Sea. *Advances in Meteorology*. 2015;**2015**:612512. DOI: 10.1155/2015/612512
- [36] Nystuen JA. An explanation of the sound generated by light rain in the presence of wind. In: Kerman BR, editor. *Natural Physical Sources of Underwater Sound*. Kluwer Academic Publishers; Dordrecht, 1993. pp. 659-668
- [37] Verfuss UK, Miller LA, Schnitzler HU. Spatial orientation in echolocating harbour porpoises (*Phocoena phocoena*). *Journal of Experimental Biology*. 2005;**208**(17):3385-3394
- [38] Doiron EE, Rouget PA, Terhune JM. Proportional underwater call type usage by Weddell seals (*Leptonychotes weddellii*) in breeding and nonbreeding situations. *Canadian Journal of Zoology*. 2012;**90**(2):237-247
- [39] Thomas JA, Kuechle VB. Quantitative analysis of Weddell seal (*Leptonychotes weddellii*) underwater vocalizations at McMurdo Sound, Antarctica. *Journal of the Acoustical Society of America*. 1982;**72**:1730-1738